Orbital Phase Resolved Analysis of the X-ray Data of FO Aqr Using XMM-Newton

Yakup PEKÖN[1,*], Şölen BALMAN[1,§]

[1] Department of Physics, Middle East Technical University
İnönü Bulvarı, Ankara, 06531, Turkey
* Email: yakup@astroa.physics.metu.edu.tr
§ Email: solen@astroa.physics.metu.edu.tr

ABSTRACT

We present the orbital-phase resolved analysis of FO Aqr data obtained with X-ray Multi-Mirror Mission (XMM–Newton),. We detect modulation of the spin pulse amplitudes over the orbital period. The amplitude variations are in phase with the orbital modulation. The spectral parameters also show changes over the orbital period. One of the absorption components increase by a factor of 4 between the orbital minimum and maximum. We interpret that this absorption arises from the bulge where accretion disk impacts the disk. The absorption due to accretion curtains which affect the spin variation plays no part in orbital variations.

INTRODUCTION

FO Aqr is a compact binary belonging to the sub-category intermediate polars (IPs) of the cataclysmic variables (CVs) which are composed of a white dwarf accreting material from a Roche lobe filling main sequence star. IPs have white dwarfs with a magnetic field of 1-10 MG. The accretion occurs through a truncated disk and via accretion curtains to the magnetic poles of the white dwarf (see Warner 2003).

FO Aqr is a well studied IP, with a constant orbital period of 4.85 hr; and white dwarf spin period of 20.9 min. which shows an erratic behaviour. The accretion happens both via a disk and stream flowing above the disk Hellier (1993). The system changes modes as disk and stream fed accretion becomes dominant. The orbital variation in the X-rays arises due to vertical structures on the disk and the accretion stream (Mukai, Ishida & Osborne 1994; Norton, Beardmore & Taylor 1996; Beardmore et al. 1998; Evans et al. 2004).

The spin pulse shape of the system is complicated, with a quasi-sinusoiadal component and a notch after a "dip" caused by the accretion curtains. The pulse profile does not change over the orbital phase however may vary between nearly sinusodial to saw-tooth shapes at different observations (Evans et al. 2004; Hellier 1993; Beardmore et al. 1998).

The X-ray spectrum of the source can be represented with a multiple plasma emission component, complex absorption and Gaussian lines (e.g. Mukai, Ishida & Osborne 1994; Yuasa et al. 2010). A broad-band spectrum using INTEGRAL/IBIS and SWIFT/XRT data also revealed a plausible blackbody component (Landi et al. 2009).

In this work, 35 ks observation of FO Aqr obtained with XMM-Newton on 12 May 2001 (OBS ID: 0009650201) is studied. EPIC pn data are used throughout the analysis due to better response. Background subtracted spectra and light curves were created with SAS tools. The light curves were then folded on the orbital and spin periods The phase resolved spectra were then extracted for each 0.1 phase interval from 0 to 1. Spectra were fitted with models using XSPEC (see Results for the models and parameters).

RESULTS

Spectral variations over the orbit

10 spectra were extracted for each 0.1 orbital phase interval. Each spectra were fitted with a composite model of simple absorption model (WABS), two partial covering absorption models (PCFABS); three plasma emission models at different temperatures (MEKAL) and a Gaussian emission line at 6.4 keV (Fe Kα) Variations of spectral parameters for each orbital phase bin were investigated. Orbital minima additionally fited with a model of a simple absorption model (WABS), a partial covering absorption model (PCFABS), a warm absorber model (WARMABS), three plasma emission models at different temperatures (MEKAL) and a Gaussian emission line at 6.4 keV (Fe Kα).

Model	Component	0.1	0.2	0.3	0.4	0.5
wabs	$N_{\rm H}$ ($\times 10^{-22}$)	$0.093^{+0.048}_{-0.034}$	$0.077^{+0.027}_{-0.035}$	$0.067^{+0.034}_{-0.027}$	$0.188^{+0.024}_{-0.020}$	$0.025^{+0.019}_{-0.015}$
pcfabs1	$N_{\rm H}$ ($\times 10^{-22}$)	$21.2^{+1.4}_{-1.3}$	$18.4^{+1.1}_{-1.0}$	$24.6^{+1.2}_{-1.1}$	$23.8^{+1.7}_{-1.5}$	$19.7^{+1.1}_{-1.1}$
	CoverFrac	$0.820^{+0.020}_{-0.020}$	$0.820^{+0.015}_{-0.015}$	$0.836^{+0.011}_{-0.011}$	$0.651^{+0.015}_{-0.015}$	$0.793^{+0.013}_{-0.013}$
pcfabs2	$N_{\rm H}$ ($\times 10^{-22}$)	$9.79^{+0.68}_{-0.63}$	$7.12^{+0.44}_{-0.40}$	$6.37^{+0.37}_{-0.34}$	$7.06^{+0.29}_{-0.27}$	$6.32^{+0.36}_{-0.33}$
	CoverFrac	$0.984^{+0.004}_{-0.007}$	$0.980^{+0.003}_{-0.005}$	$0.980^{+0.003}_{-0.004}$	$0.980^{+0.002}_{-0.002}$	$0.980^{+0.003}_{-0.002}$
MEKAL1	kT	$0.117^{+0.013}_{-0.015}$	$0.159^{+0.025}_{-0.027}$	$0.165^{+0.029}_{-0.030}$	$0.125^{+0.010}_{-0.010}$	$0.180^{+0.022}_{-0.022}$
	Norm ($\times 10^{-3}$)	$8.05^{+3.23}_{-3.23}$	$3.95^{+1.43}_{-1.43}$	$3.61^{+1.36}_{-1.36}$	$7.12^{+1.70}_{-1.70}$	$3.65^{+0.75}_{-0.75}$
MEKAL2	kT	$6.87^{+5.00}_{-4.17}$	$2.25^{+0.57}_{-0.51}$	$2.71^{+0.71}_{-0.57}$	$8.19^{+3.51}_{-3.00}$	$3.01^{+0.67}_{-0.48}$
	Norm ($\times 10^{-5}$)	$1.72^{+0.84}_{-0.84}$	$2.63^{+1.25}_{-1.25}$	$3.01^{+1.01}_{-1.01}$	$2.49^{+0.86}_{-0.86}$	$3.05^{+0.78}_{-0.78}$
MEKAL3	kT	$44.7^{+18.4}_{-17.6}$	$27.2^{+10.2}_{-7.0}$	$21.3^{+6.9}_{-3.6}$	$37.6^{+9.9}_{-8.4}$	$40.8^{+12.5}_{-9.6}$
	Norm ($\times 10^{-3}$)	$5.62^{+0.17}_{-0.17}$	$5.70^{+0.15}_{-0.15}$	$6.85^{+0.17}_{-0.17}$	$6.61^{+0.14}_{-0.14}$	$5.59^{+0.14}_{-0.14}$
Gaussian	line centre (keV)	$6.38^{+0.04}_{-0.03}$	$6.41^{+0.03}_{-0.03}$	$6.37^{+0.05}_{-0.04}$	$6.39^{+0.02}_{-0.03}$	$6.31^{+0.05}_{-0.06}$
	σ	$0.052^{+0.073}_{-0.052}$	$0.040^{+0.057}_{-0.040}$	$0.060^{+0.098}_{-0.060}$	$0.001^{+0.067}_{-0.001}$	$0.086^{+0.069}_{-0.061}$
	Norm ($\times 10^{-5}$)	$0.92^{+0.33}_{-0.33}$	$0.96^{+0.30}_{-0.30}$	$0.88^{+0.35}_{-0.35}$	$1.24^{+0.31}_{-0.31}$	$1.09^{+0.34}_{-0.34}$
	χ^2_ν (d.o.f.)	0.80 (83)	0.82 (76)	1.08 (75)	1.25 (75)	0.83 (73)

Model	Component	0.6	0.7	0.8	0.9	1.0
wabs	$N_{\rm H}$ ($\times 10^{-22}$)	$0.021^{+0.019}_{-0.016}$	$0.145^{+0.024}_{-0.020}$	$0.052^{+0.014}_{-0.012}$	$0.079^{+0.030}_{-0.023}$	$0.152^{+0.041}_{-0.029}$
pcfabs1	$N_{\rm H}$ ($\times 10^{-22}$)	$21.7^{+1.3}_{-1.2}$	$16.5^{+1.1}_{-1.0}$	$26.5^{+1.3}_{-1.3}$	$26.2^{+1.6}_{-1.5}$	$20.0^{+2.6}_{-2.0}$
	CoverFrac	$0.731^{+0.013}_{-0.013}$	$0.697^{+0.013}_{-0.013}$	$0.776^{+0.010}_{-0.010}$	$0.828^{+0.016}_{-0.016}$	$0.689^{+0.041}_{-0.041}$
pcfabs2	$N_{\rm H}$ ($\times 10^{-22}$)	$5.78^{+0.28}_{-0.26}$	$3.75^{+0.16}_{-0.15}$	$6.37^{+0.27}_{-0.25}$	$11.26^{+0.79}_{-0.74}$	$17.45^{+1.20}_{-1.11}$
	CoverFrac	$0.980^{+0.003}_{-0.002}$	$0.980^{+0.003}_{-0.003}$	$0.980^{+0.001}_{-0.002}$	$0.980^{+0.003}_{-0.004}$	$0.980^{+0.004}_{-0.005}$
MEKAL1	kT	$0.199^{+0.024}_{-0.023}$	$0.147^{+0.013}_{-0.013}$	$0.128^{+0.009}_{-0.009}$	$0.160^{+0.023}_{-0.023}$	$0.103^{+0.009}_{-0.011}$
	Norm ($\times 10^{-3}$)	$3.68^{+0.78}_{-0.78}$	$33.06^{+7.90}_{-7.90}$	$5.72^{+1.00}_{-1.00}$	$3.17^{+0.98}_{-0.98}$	$5.36^{+2.07}_{-2.07}$
MEKAL2	kT	$2.73^{+0.90}_{-0.67}$	$1.71^{+0.37}_{-0.27}$	$6.35^{+4.46}_{-3.34}$	$1.18^{+0.34}_{-0.19}$	$2.17^{+0.57}_{-0.50}$
	Norm ($\times 10^{-5}$)	$2.80^{+1.15}_{-1.15}$	$4.00^{+1.07}_{-1.07}$	$2.25^{+1.02}_{-1.02}$	$2.06^{+1.16}_{-1.16}$	$1.90^{+0.96}_{-0.96}$
MEKAL3	kT	$28.6^{+10.2}_{-6.8}$	$30.6^{+8.0}_{-6.6}$	$14.8^{+1.9}_{-1.2}$	$32.6^{+17.8}_{-10.5}$	$69.1^{+15.0}_{-15.0}$
	Norm ($\times 10^{-3}$)	$6.48^{+0.15}_{-0.15}$	$5.42^{+0.12}_{-0.12}$	$7.30^{+0.16}_{-0.16}$	$5.55^{+0.18}_{-0.18}$	$3.57^{+0.15}_{-0.15}$
Gaussian	line centre (keV)	$6.36^{+0.03}_{-0.03}$	$6.36^{+0.04}_{-0.04}$	$6.36^{+0.03}_{-0.04}$	$6.42^{+0.03}_{-0.03}$	$6.39^{+0.03}_{-0.03}$
	σ	$0.075^{+0.047}_{-0.042}$	$0.114^{+0.053}_{-0.038}$	$0.053^{+0.054}_{-0.053}$	$0.036^{+0.041}_{-0.036}$	$0.070^{+0.069}_{-0.070}$
	Norm ($\times 10^{-5}$)	$1.79^{+0.37}_{-0.37}$	$1.76^{+0.37}_{-0.37}$	$1.08^{+0.33}_{-0.33}$	$1.07^{+0.32}_{-0.32}$	$1.15^{+0.33}_{-0.33}$
	χ^2_ν (d.o.f.)	1.07 (80)	0.73 (83)	0.74 (66)	0.82 (72)	0.90 (69)

Spectral parameters derived from each orbital phase of 0.1 in the 0.3-10 keV range. The given errors correspond to 2 σ confidence level for a single parameter.

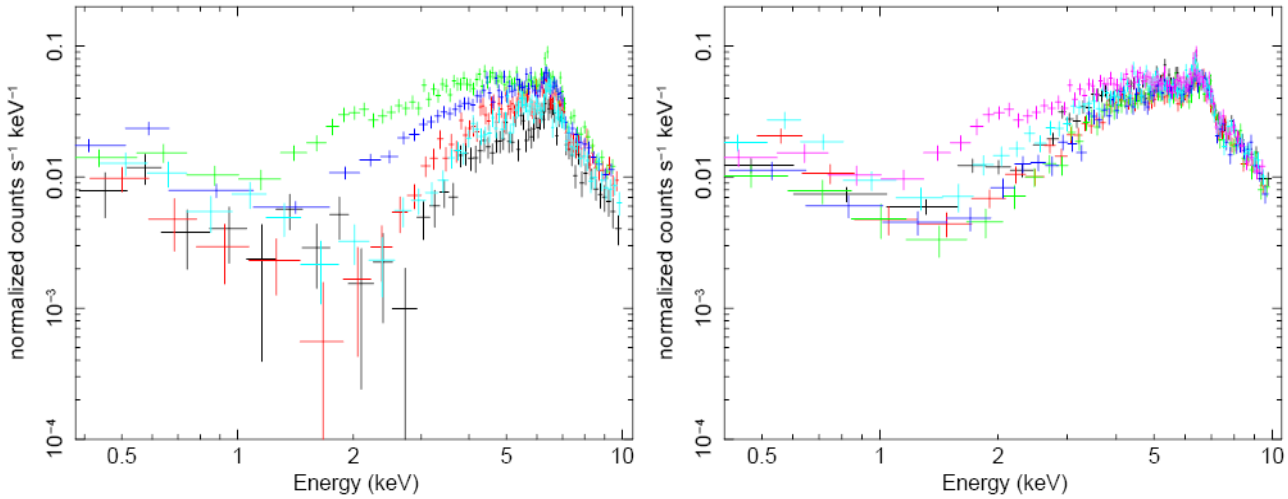

The orbital-phase resolved spectra of FO Aqr for each 0.1 phase bin interval. The left-hand panel shows phases 0.6 (green) 0.7 (dark-blue), 0.8 (red), 0.9 (black) and 1.0 (light-blue). The right-hand panel shows the phases 0.8 (purple-pink) and the rest of the phases 0.1-0.5. Notice the spectral differences on the left-hand side during orbital minima and how the spectra are different for the rest of the phases

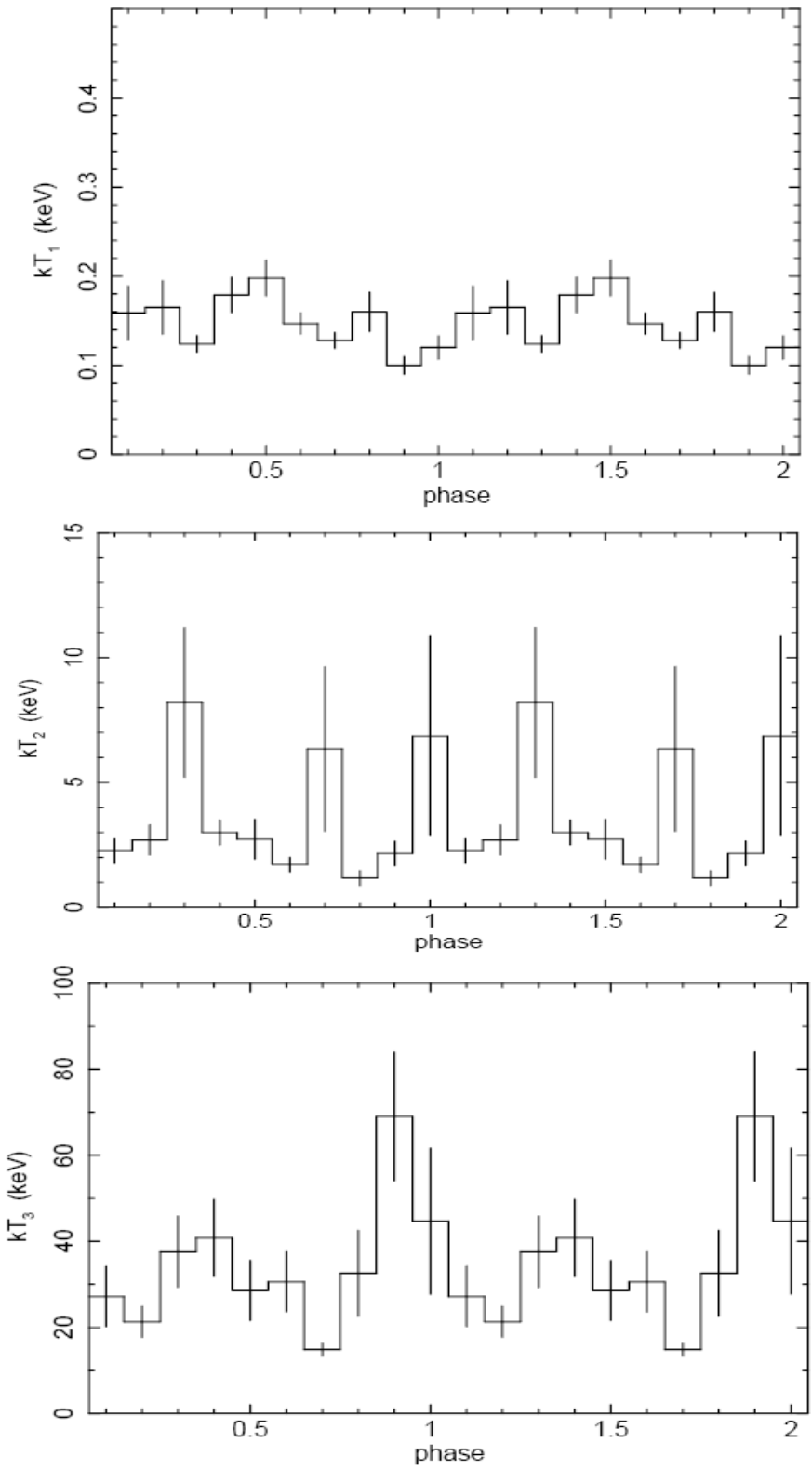

The variation of plasma temperatures of three different MEKAL components over the orbital phase.

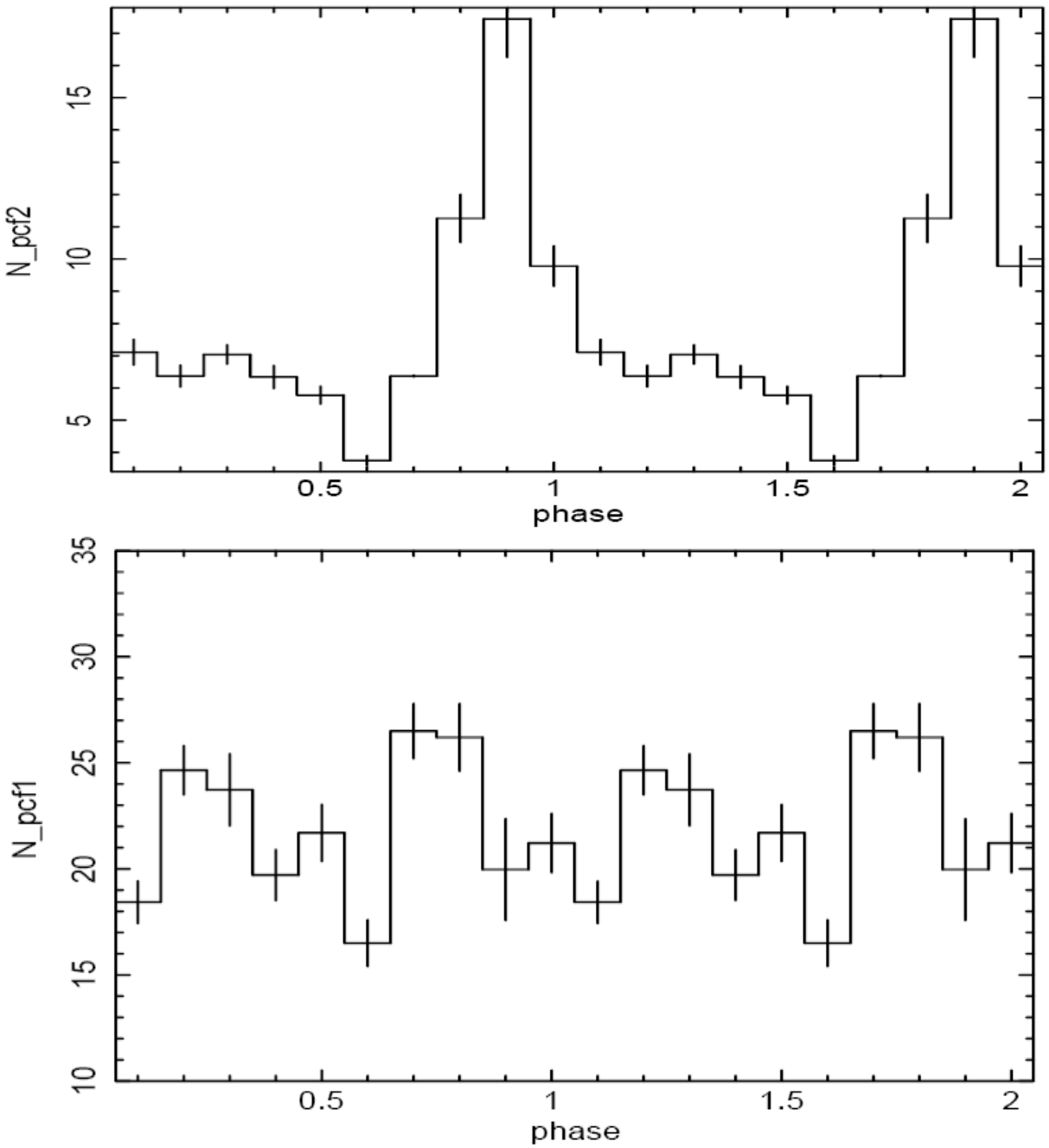

The variation of N_H parameter of the partial covering absorber components (pcfabs1 and pcfabs2) over the orbital period

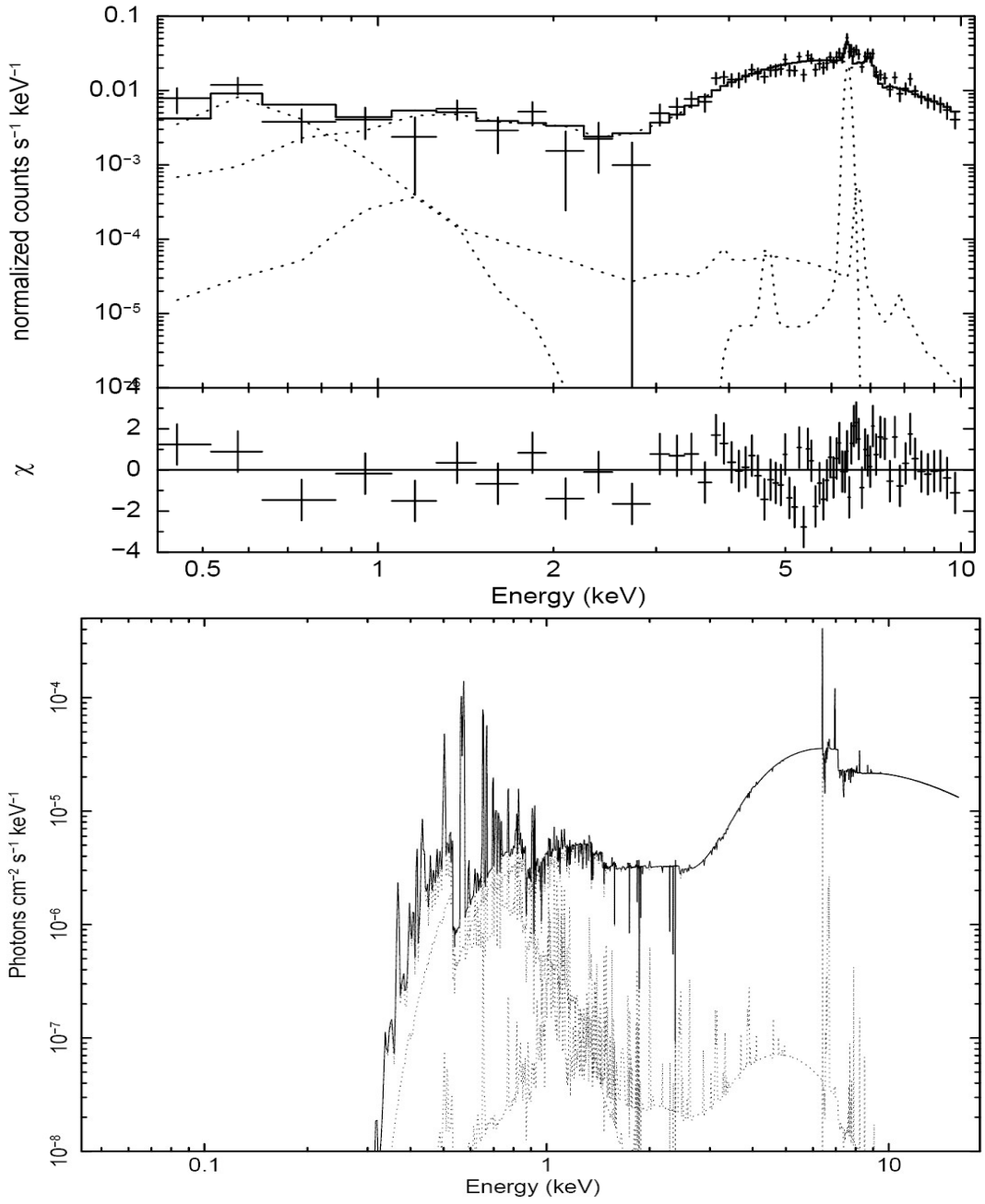

The composite model with warm absorber fitted to the orbital minima on the left. On the right, only the model itself is plotted.

Spin modulations over the orbit

10 light curves were extracted for each 0.1 orbital phase interval. Extracted light curves were then folded over the spin period. Each folded light curve were fitted with a simple sine curve. Semi-amplitude variations over the orbital phase were investigated.

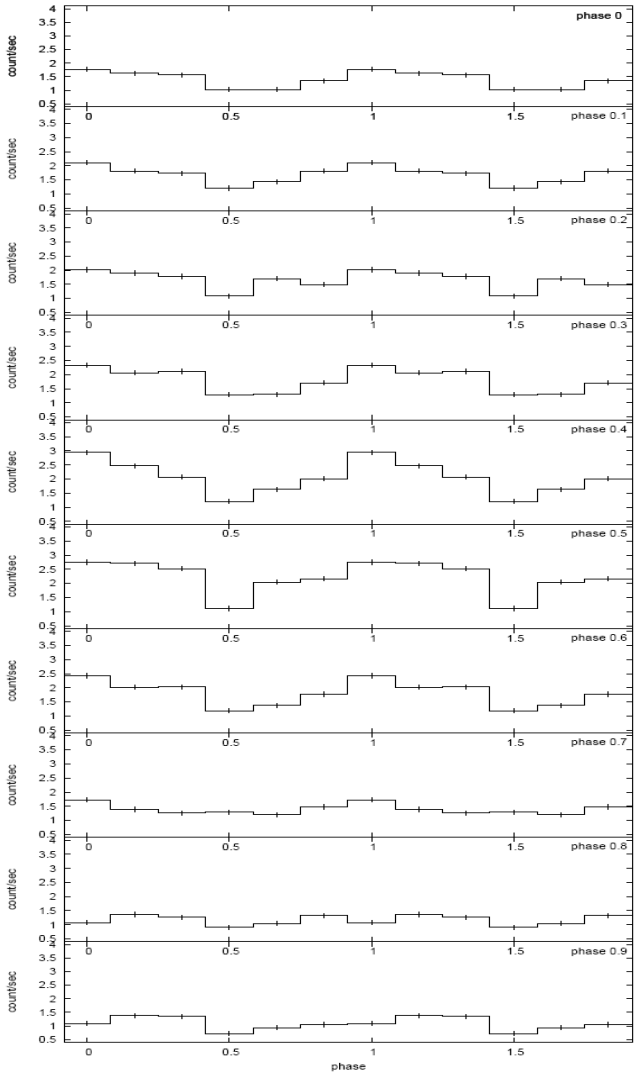

The spin pulse profile of FO Aqr for each 0.1 orbital phase interval.

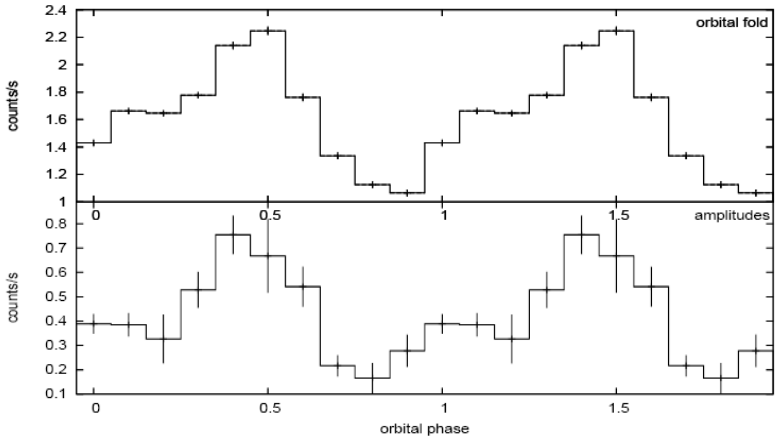

The semi-amplitude variation of the spin pulses (below), together with the orbital flux variation (above).

DISCUSSION

The source shows spectral variability over the orbital period. One distinct variation is seen in N_H parameter of the second absorption component (pcfabs2). It shows direct correlation with the orbital flux and the value changes by a factor of four, going from 3.75×10^{22} cm^{-2} to 17.45×10^{22} cm^{-2} from orbital maximum to orbital minimum. The other absorption component (pcfabs1) shows no variation with the orbital motion with higher values than the second component ranging between 16.5-26.5 $\times 10^{22}$ cm^{-2}. Hence it can be inferred that the varying absorption component associates with a bulge on the disk and/or the hot spot. This approach is consistent with Hellier (1993) where a bulge on the disk is accounted for. The other component can be associated to the absorption due to spin (i.e. From the accretion curtains), which explains the constant behaviour of the absorption parameter. Since the spin period is significantly smaller than the orbital period, the absorption effects due to spin average out.

Another significantly varying parameter is the temperature of the third plasma emission. While the other two plasma components show no distinct variation, it maximizes at the orbital minimum. This plasma component is the one with the highest temperature, hence the spectrum hardens during the orbital minima, supporting the absorption from bulge on the disk.

The orbital minimum spectrum can be represented with a warm absorber model with a χ_ν^2 of 1.4 with values log $\xi = 2.2$ ($\xi = L/n_e r^2$) and $N_H = 6.5 \times 10^{22}$ cm^{-2} which is the ionized absorption column. The above mentioned bulge on the disk or the hot spot can be the source of this warm absorber in the system.

The spin pulse profiles of the system does not change with the orbital phase. They all have the same sinusoidal shape with minimum around phase 0.5 and maximum around phase 1.0. However, the semi-amplitude of the spin variations change with the orbital motion changing from 36% at orbital maximum to 14% at orbital minimum. This again shows that we can clearly distinguish the absorption effects due to orbital motion from the spin.

REFERENCES

Hellier C., 1993, MNRAS, 265, 35
Beardmore A. P. et al., 1998, MNRAS 297, 337
Warner B., 2003, Cataclysmic Variable Stars. Cambridge Univ. Press, Cambridge
Mukai K., Ishida M., Osborne J.P., 1994, PASJ, 46, 87
Norton A.J, Beardmore A.P., Taylor P., 1996, MNRAS, 280, 937
Evans P.A. Et al., 2004, 349, 715
Yuasa T. et al., 2010, A&A, 520, 25
Landi R. et al., 2009, MNRAS, 392, 630

* We acknowledge support from TÜBİTAK, The Scientific and Technological Research Council of Turkey, through project 108T735.